

# Colloidal gelation, percolation and structural arrest

A. de Candia <sup>a,b</sup>, E. Del Gado<sup>a,b</sup>, A. Fierro <sup>a,c</sup>, N. Sator <sup>d</sup>, and A. Coniglio <sup>a,c</sup>

<sup>a</sup> Dipartimento di Scienze Fisiche and INFN Sezione di Napoli,  
Università di Napoli “Federico II”, via Cintia 80126 Napoli, Italy

<sup>b</sup> CNISM Napoli

<sup>c</sup> Coherentia CNR-ENIM and

<sup>d</sup> Laboratoire de Physique Théorique des Liquides Université Pierre et Marie Curie  
UMR CNRS 7600 Case 121, 4 Place Jussieu 75252 Paris Cedex 05, France

(Dated: July 8, 2019)

By means of molecular dynamics, we study a model system for colloidal suspensions where the interaction is based on a competition between attraction and repulsion. At low temperatures the relaxation time first increases as a power law as a function of the volume fraction and then, due to the finite lifetime of the bonded structures, it deviates from this critical behavior. We show that colloidal gelation at low temperatures and low volume fractions is crucially related to the formation of spanning long living cluster, as we suggested in the last few years. Besides agreeing with experimental findings in different colloidal systems, our results shed new light on the different role played by the formation of long living bonds and the crowding of the particles in colloidal structural arrest. PACS: 82.70.Dd, 64.60.Ak, 82.70.Gg

In attractive colloids a rich phenomenology is found in the temperature - volume fraction plane [1]-[7]. At high temperature a hard sphere glass transition occurs at a volume fraction,  $\phi \simeq 0.57$ . By decreasing the temperature, at high volume fraction, the effect of the short range attraction produces an attractive glass line with a reentrant line well described in the framework of the mode coupling theory [8, 9], and confirmed by experiments. At low temperature and increasing the volume fraction a much more complex situation arises [3], [11]-[16], characterized by a cluster phase followed by a kinetic arrest with viscoelastic properties very similar to those found in polymer gelation.

One of the important problems is to understand the mechanism which gives rise to colloidal gelation. When phase separation does not occur, colloidal gelation has been interpreted in terms of cluster mode coupling theory [13] or Wigner glass [15]. In contrast to these approaches, we have suggested that at low volume fraction and low temperature, percolation phenomena play a crucial role in colloidal gelation characterized by the presence of a spanning cluster of bonded particles [14, 17] as also found in recent experiments [18]. Of course, at high enough temperature and high volume fraction, one expects a structural arrest due essentially to the hard sphere part of the potential. At intermediate values of temperature and volume fractions, molecular dynamical studies have shown the occurrence of colloidal gelation phenomena characterized by a structural arrest, on average well described by the mode coupling theory of attractive glasses [10]. Interestingly, the system is dynamically heterogeneous: The set of all particles can be partitioned in two subsets made of slow and fast particles and structural arrest occurs close to the onset of a spanning cluster of only the subset of slow particles [10]. One may ask the question whether the same scenario for colloidal gelation can be smoothly extended from this intermediate regime

to the low volume fraction region. In this letter, by using a molecular dynamics simulations of a DLVO-type potential [19] for charged colloidal systems, we give evidence of a clear crossover from the low volume fraction regime to the intermediate regime. In the first regime we find the bond lifetime much larger than the structural relaxation time. As a consequence, dynamically, the clusters behave as made of permanent bonds as in chemical gelation, and the regime is dominated by the dynamics of such clusters. Increasing  $\phi$ , when these two time scales become comparable, the structural relaxation begins to be affected also by the crowding of the particles, and a clear crossover to a new glassy regime is found. Interestingly enough such crossover has also been found in some micellar systems at rather high volume fraction [17, 20], suggesting a common mechanism in both systems.

We consider a system of  $N = 10000\phi$  particles, with  $\phi = 0.08-0.25$ , interacting via a DLVO-type potential, which contains a Van der Waals type interaction plus an effective repulsion due to the presence of charges:

$$V(r) = \epsilon \left[ a_1 \left( \frac{\sigma}{r} \right)^{36} - a_2 \left( \frac{\sigma}{r} \right)^6 + a_3 e^{-\lambda(\frac{r}{\sigma}-1)} \right], \quad (1)$$

where  $a_1 = 2.3$ ,  $a_2 = 6$ ,  $a_3 = 3.5$ , and  $\lambda = 2.5$  [21]. With these parameters the repulsion term dominates the Van der Waals attraction at long range, providing a short range attraction and a long range repulsive barrier. The effective repulsion in the potential prevents the liquid-gas phase separation and stabilize the size of the clusters, as expected [11]. The potential is truncated and shifted at a distance of  $3.5\sigma$ . To mimic the colloidal dynamics, we performed molecular dynamics simulations at constant temperature. Equations of motion were solved in the canonical ensemble (with a Nosé-Hoover thermostat) using a velocity Verlet algorithm [22] with a time step of  $0.001t_0$  (where  $t_0 = \sqrt{\frac{m\sigma^2}{\epsilon}}$  and  $m$  is the mass of the

particles). We equilibrate the system at temperatures  $k_B T = 0.2, 0.23, 0.25\epsilon$  and  $\phi$  increasing from 0.07 to 0.23.

Here we analyze the structure and the dynamics by varying the temperature and volume fraction. We calculate first the static structure factor,  $S(k)$ , and the cluster size distribution,  $n(s)$ , where two particles are linked if their relative distance is smaller than the local maximum of the potential [23].

At low temperatures, i.e. when the kinetic energy becomes smaller than the repulsive barrier, and low volume fractions, the static structure factor,  $S(k)$ , displays a peak around  $k_0 \simeq 2$  (see Fig. 1). This feature is due to the fact that the competing short range attraction and long range repulsion produce stable clusters of a typical size. The presence of a typical size is also manifested in the cluster size distribution,  $n(s)$ , plotted in Fig. 2 at  $k_B T = 0.2\epsilon$  and  $\phi = 0.13$ . It is interesting to observe the secondary peak due to the fusion of two stable clusters. By increasing the volume fraction  $\phi$ , a spanning cluster appears at  $\phi = 0.16$  for  $k_B T = 0.2\epsilon$ , and the cluster size distribution typically displays a power law decay with an exponent  $\tau \simeq 2.18$ , consistent with the random percolation model [24]. In Fig. 3 we show the dependence of the cluster size,  $s$ , on its radius,  $r$ , at  $\phi_p$ : The data correspond to a compact structure for clusters of dimension  $s \lesssim 10$  and radius  $r \lesssim 1$ , a fractal dimensionality  $d_f \simeq 1.2$  on intermediate length scales, and a crossover to  $d_f \simeq 2.5$  at larger length scales. These results suggest that at low volume fraction compact stable clusters form with typical size  $s \simeq 10$  and radius  $r \simeq 1$ . By increasing the volume fraction a residual attractive interaction between the clusters produces tube-like structures with fractal dimension  $d_f \simeq 1.2$  up a size  $s \sim 60$ . By further increasing the volume fraction these structures coalesce to build a random percolating network. For the temperature here studied the percolation threshold  $\phi_p$  is weakly dependent on the temperature,  $0.16 \lesssim \phi_p \lesssim 0.17$ .

A preliminary study of this model was published in Ref. [14] and these results were presented in the meeting “Dynamical arrest”, hold in Bad Gastein in January 2005. This analysis has been lately developed in Ref. [16], where using a qualitatively similar interaction potential the authors have found again the behavior shown in Fig.s 2 and 3, and stressed the role of percolation. Interestingly they have also shown that this model is actually able to reproduce the local order typically observed in the experimental system [18].

In order to study the relaxation dynamics, we calculate different time autocorrelation functions at equilibrium. In Fig. 4 the incoherent scattering functions,  $F_s(k, t)$ , are plotted for  $k \simeq 1.88$ ,  $k_B T = 0.25\epsilon$  and different  $\phi$ . From these functions we extract a characteristic relaxation time,  $\tau_\alpha$ , defined by  $F_s(k, \tau_\alpha) = 0.1$ , plotted in Fig. 6.

We also study the time correlation of the clusters in

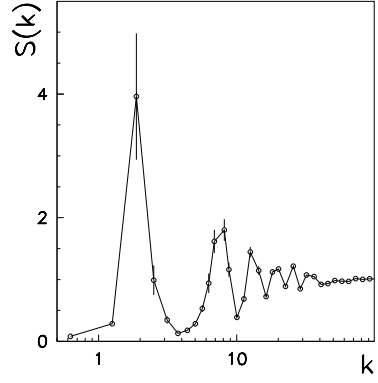


FIG. 1: The static structure factor,  $S(k)$ , at  $k_B T = 0.2\epsilon$  and  $\phi = 0.13$ , displays a peak around  $k_0 \simeq 2$ .

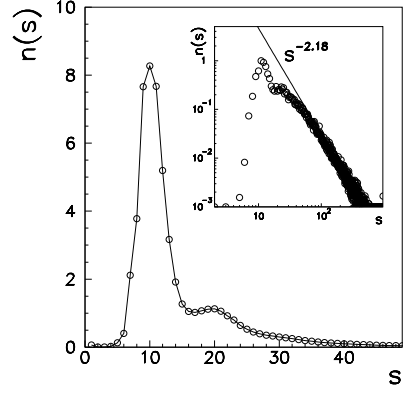


FIG. 2: **Main frame:** the cluster size distribution,  $n(s)$ , at  $k_B T = 0.2\epsilon$  and  $\phi = 0.13$ , displays a peak around an optimum cluster size. **Inset:** At  $\phi = 0.16 \simeq \phi_p$ , a power law tail appears.

terms of the time autocorrelation functions of the bonds,  $B(t)$ , which are plotted in Fig. 5.

The function  $B(t)$  is defined as

$$B(t) = \frac{\sum_{ij} [\langle n_{ij}(t) n_{ij}(0) \rangle - \langle n_{ij} \rangle^2]}{\sum_{ij} [\langle n_{ij} \rangle - \langle n_{ij} \rangle^2]}, \quad (2)$$

where  $n_{ij}(t) = 1$  if particles  $i$  and  $j$  are linked at time  $t$ ,  $n_{ij}(t) = 0$  otherwise. The data show that, differently from the behavior of  $F_s(k, t)$ , the bond relaxation does not change much below the percolation threshold,  $\phi_p$ , and instead it becomes slower and slower above the percolation threshold. From these functions, we obtain the bond lifetime,  $\tau_b$ , as  $B(\tau_b) = 0.1$ . In Fig. 6  $\tau_b$  is compared with  $\tau_\alpha$ . The data show that, at low volume fractions, the bond lifetime is much larger than the density relax-

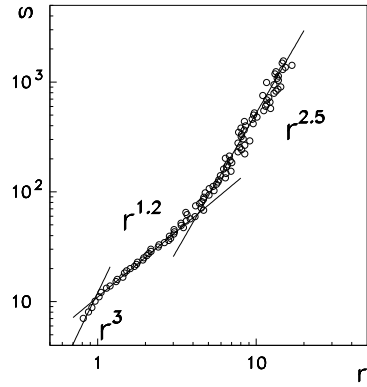


FIG. 3: The cluster size,  $s$ , as a function of the radius,  $r$ , at  $k_B T = 0.2\epsilon$  and  $\phi = 0.16 \simeq \phi_p$ : While at very small scales clusters are compact, on intermediate length scales the dependence suggests the presence of very thin and chain structures made up by clusters of typical size  $s \lesssim 10$ ; It crosses to a random percolation type of structure over larger length scales.

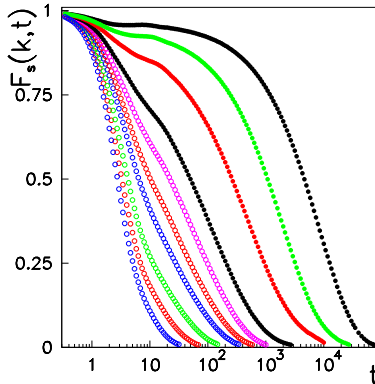


FIG. 4: (color online). The incoherent scattering function,  $F_s(k, t)$ , for  $k_B T = 0.25\epsilon$  and  $\phi = 0.08, 0.10, 0.12, 0.14, 0.15, 0.16, 0.17, 0.19, 0.21, 0.23$  (from left to right). Empty circles in figure correspond to values of  $\phi < \phi_p$ .

ation time and in this region  $\tau_\alpha$  can be fitted by a power law. This result can be understood by considering that the system dynamically behaves as made of permanent clusters and the structural relaxation is directly related to the size of the clusters, like in chemical gelation. At higher volume fraction close to the percolation threshold, the relaxation time and the bond lifetime eventually become of the same order of magnitude and one observes a deviation from the power law critical behavior.

Within this scenario, the percolation of long-living structures is the mechanism which produces the enhancement of the structural relaxation time at low volume frac-

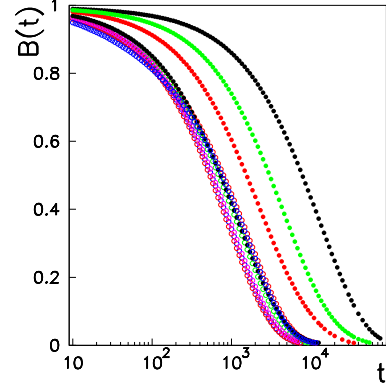


FIG. 5: (color online). The bond correlation function,  $B(t)$ , for  $k_B T = 0.25\epsilon$  and  $\phi = 0.08, 0.10, 0.12, 0.14, 0.15, 0.16, 0.17, 0.19, 0.21, 0.23$  (from left to right). Empty circles in figure correspond to values of  $\phi < \phi_p$ .

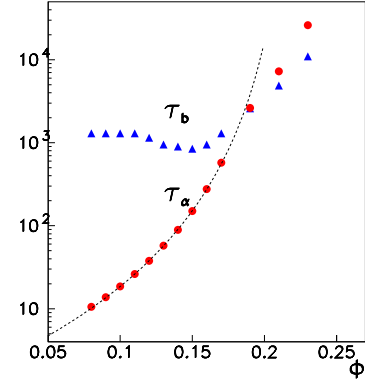


FIG. 6: (color online). The bond lifetime,  $\tau_b$ , and the relaxation time,  $\tau_\alpha$ , (in units of MD steps) as a function of the volume fraction  $\phi$  at  $k_B T = 0.25\epsilon$ . The curve in figure is a power law fit,  $(\phi_c - \phi)^{-\gamma}$ , with  $\phi_c \simeq 0.22$  and  $\gamma \simeq 4.0$ .

tion: Close to the percolation threshold,  $\tau_\alpha$  increases fast enough to reach the scale of the bond lifetime, and the dynamics crosses over to the glassy regime.

In fact in this region on the time scale of the structural relaxation time, the bonds cannot be considered as permanent anymore. This explains the crossover to a glassy regime, in which the structural relaxation time depends on the bond finite lifetime and the crowding of the particles.

At higher temperature when the bond lifetime does not play any role, structural arrest is only due to the hard sphere component of the potential.

By decreasing the temperature we find that the critical regime becomes more extended, due to the increase

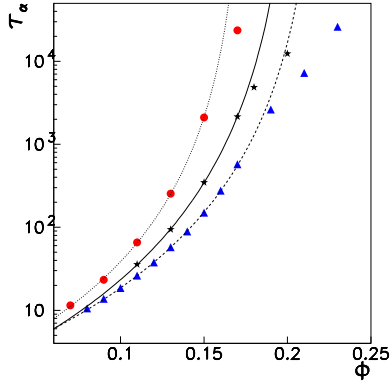


FIG. 7: (color online). The relaxation time,  $\tau_\alpha$ , as a function of the volume fraction,  $\phi$ , for different temperatures,  $T = 0.25, 0.23, 0.2$  (from right to left). The curves are power laws,  $(\phi_c - \phi)^{-\gamma}$ , where respectively  $\phi_c \simeq 0.22$  and  $\gamma \simeq 4.0$ ,  $\phi_c \simeq 0.21$  and  $\gamma \simeq 4.3$ , and  $\phi_c \simeq 0.17$  and  $\gamma \simeq 3.7$ . The percolation threshold is weakly dependent on the temperature,  $0.16 \lesssim \phi_p \lesssim 0.17$ .

of the bond lifetime (see Fig. 7), and the critical volume fraction  $\phi_c$  tends to the percolation threshold  $\phi_p$ . Therefore at very low temperatures we expect the structural arrest to coincide with the onset of a spanning cluster on the time scale of the numerical simulations, in agreement with previous results [14] and recent experiments[18].

In order to further understand and characterize the crossover region, we have calculated the dynamic susceptibility, defined as the fluctuations of  $F_s(k, t)$  [25]:

$$\chi_4(k, t) = N(\langle F_s(k, t)^2 \rangle - \langle F_s(k, t) \rangle^2). \quad (3)$$

Similar quantities, largely studied in glassy systems (see Refs. [26, 27]), are related to the presence of dynamic heterogeneities, spatial correlations between particles that move faster than the average. In Fig. 8,  $\chi_4(k, t)$  is plotted as function of  $t$ , for  $k \simeq 1.88$ ,  $k_B T = 0.25\epsilon$  and different values of  $\phi$ . We find that  $\chi_4(k, t)$  exhibits a maximum at time  $t^*$ , which first increases and then decreases signalling the presence of a crossover as clearly shown in Fig. 9, where the time,  $t^*$ , and the maximum value,  $\chi_4(k, t^*)$ , are plotted as a function of the volume fraction: At low volume fraction they both follow a power law diverging, whereas a deviation from this critical behavior appears at volume fraction higher than the percolation threshold.

The presence of a maximum at a time  $t^*$ , increasing together with the height of the maximum was recently found in experiments on colloidal gels as colloidal gelation was approached [28].

In conclusions in our model the presence of two well separated time scales at low temperature and low volume

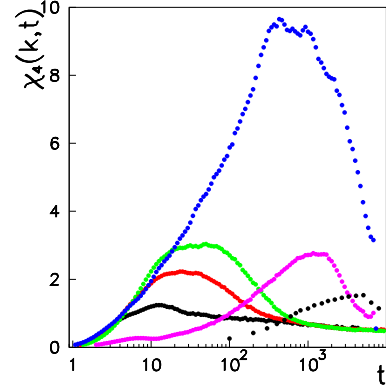


FIG. 8: (color online). The dynamic susceptibility,  $\chi_4(k, t)$ , for  $k \simeq 1.88$ ,  $k_B T = 0.25\epsilon$  and  $\phi = 0.08, 0.13, 0.15, 0.17, 0.21, 0.23$  (from left to right).

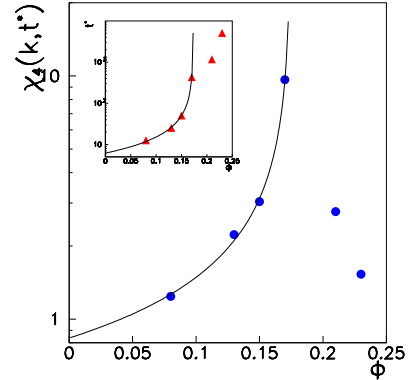


FIG. 9: (color online). **Main frame** The maximum value of the dynamic susceptibility,  $\chi_4(k, t^*)$ , as a function of the volume fraction,  $\phi$ , at  $k_B T = 0.25\epsilon$ . The curve in figure is a power law fit,  $(\phi_c - \phi)^{-\gamma}$ , with  $\phi_c \simeq 0.17$  and  $\gamma \simeq 0.68$ . **Inset** The time,  $t^*$ , (in units of MD steps) as a function of the volume fraction,  $\phi$ , at  $k_B T = 0.25\epsilon$ . The curve in figure is a power law fit,  $(\phi_c - \phi)^{-\gamma}$ , with  $\phi_c \simeq 0.17$  and  $\gamma \simeq 1.0$ .

fraction originates a colloidal gelation related to the formation of persistent structures: Increasing the volume fraction the two time scales become comparable and a crossover from a gel-like behavior to a glass-like one is found.

This work has been partially supported by the Marie Curie Fellowship HPMF-CI2002-01945 and Reintegration Grant MERG-CT-2004-012867, EU Network Number MRTN-CT-2003-504712, MIUR-PRIN 2004, MIUR-FIRB 2001, CRdC-AMRA, INFM-PCI.

---

[1] W. C. Poon *et al.*, *Physica A* **235**, 110 (1997).

[2] V. Trappe *et al.*, *Nature* **411**, 772 (2001).

[3] P. N. Segré *et al.*, *Phys. Rev. Lett.* **86**, 6042 (2001).

[4] A. D. Dinsmore and D. A. Weitz, *J. Phys. : Condens. Matter* **14**, 7581 (2002).

[5] A. Stradner *et al.* *Nature* **432**, 492 (2004).

[6] V. Prasad *et al.*, *Faraday Discussions* **123**, 1-12 (2003).

[7] H. Gang *et al.*, *Phys. Rev. E* **59**, 715 (1999); F. Mallamace *et al.*, *Phys. Rev. Lett.* **84**, 5431 (2000); S. H. Chen, W. R. Chen, F. Mallamace, *Science* **300**, 619 (2003).

[8] L. Fabbian *et al.*, *Phys. Rev. E* **59**, R1347 (1999); J. Bergenholz, M. Fuchs, and Th. Voigtmann, *J. Phys. : Condens. Matter* **12**, 6575 (2000).

[9] A.M. Puertas, M. Fuchs and M.E. Cates, *Phys. Rev. E* **67**, 031406 (2003).

[10] A.M. Puertas, M. Fuchs and M.E. Cates, *cond-mat/0409740*.

[11] J. Groenewold and W. K. Kegel, *J. Phys. Chem. B* **105**, 11702 (2001).

[12] F. Sciortino, *Nature Materials, News and Views* **1**, 145 (2002).

[13] K. Kroy, M. E. Cates, and W. C. K. Poon, *Phys. Rev. Lett.* **92**, 148302 (2004).

[14] A. Coniglio *et al.*, *J. Phys. C: Condens. Matter* **16**, S4831 (2004).

[15] F. Sciortino *et al.*, *Phys. Rev. Lett.* **93**, 055701 (2004).

[16] F. Sciortino, P. Tartaglia and E. Zaccarelli, *cond-mat/0505453*.

[17] E. Del Gado *et al.*, *Europhys. Lett.* **63**, 1 (2003); E. Del Gado *et al.*, *Phys. Rev. E* **69**, 051103 (2004).

[18] A.I. Campbell *et al.*, *Phys. Rev. Lett.* *in press*.

[19] J.N. Israelachvili, "Intermolecular and surface forces", Academic press (London) 1985; J. C. Crocker and D. G. Grier, *Phys. Rev. Lett.* **73**, 352 (1994).

[20] F. Mallamace *et al.*, *cond-mat/0505723*.

[21] The potential  $V(r)$ , eq. (1), essentially coincides with a Lennard-Jones interaction plus a repulsive Yukawa potential  $\epsilon \left[ A_1 \left( \frac{a}{r} \right)^{36} - A_2 \left( \frac{a}{r} \right)^6 + a \frac{e^{-r/\xi}}{\sigma} \right]$ , with  $A_1 = 3.56$ ,  $A_2 = 7.67$ ,  $a = 36.79$  and  $\xi = 0.49\sigma$ .

[22] W. G. Hoover, *Phys. Rev. A* **31**, 1695 (1985); M.P. Allen and D.J. Tildesley, "Computer Simulation of Liquids", Clarendon Press : Oxford University Press (1987).

[23] At low temperatures, such as the temperatures studied in this paper, this definition is practically equivalent to the Hill definition adopted in first paper of Ref. [14].

[24] D. Stauffer and A. Aharony *Introduction to percolation theory*, Taylor and Francis, London (1992).

[25] C. Toninelli *et al.* *cond-mat/0412158*.

[26] S. Franz *et al.*, *Philos. Mag. B* **79**, 1827 (1999). C. Donati, S. Franz, S. C. Glotzer and G. Parisi, *J. Non-cryst. Solids*, **307**, 215 (2002).

[27] W. Kob *et al.*, *Phys. Rev. Lett.* **79**, 2827 (1997); C. Donati, S.C. Glotzer and P.H Poole, *Phys. Rev. Lett.* **82**, 5064 (1999); C. Donati *et al.*, *Phys. Rev. E* **60**, 3107 (1999).

[28] A. Duri *et al.*, *cond-mat/0410150*; L. Cipelletti *et al.*, in preparation.